Development of a Mixed-Effect Pharmacokinetic Model for Vehicle Modulated *In Vitro* Transdermal Flux of Topically Applied Penetrants

JASON T. CHITTENDEN,[1] JAMES D. BROOKS,[1] JIM E. RIVIERE[2]

[1]Center for Chemical Toxicology Research and Pharmacokinetics, College of Veterinary Medicine, North Carolina State University, Raleigh, North Carolina 27607

[2]College of Veterinary Medicine, Coles 207, Department of Anatomy and Physiology, Kansas State University, Manhattan, Kansas 66506-5802

Received 21 July 2013; revised 27 December 2013; accepted 3 January 2014

Published online 30 January 2014 in Wiley Online Library (wileyonlinelibrary.com). DOI 10.1002/jps.23862

ABSTRACT: Transient flux profiles from *in vitro* flow-through cell experiments exhibit different characteristics depending upon the properties of the penetrants and vehicle mixtures applied. To enable discrimination of the chemical properties contributing to these differences, a consistent mathematical model should first be developed. A mixed effects modeling framework was used so that models can be estimated with as few parameters as possible, while also quantifying variability and accounting for correlation in the data. The models account for diffusion and binding within the membrane as well as dynamics on the diffusion coefficient. The models explain key features of the data, such as: lag time, sharp peaks in flux, two terminal phases, and low flux profiles. The models with dynamic diffusivity fit the data better than those without—particularly the sharp peaks. The significance of changing diffusivity over time suggests that vehicle effects are transient and are more accurately estimated when dynamics are modeled. © 2014 Wiley Periodicals, Inc. and the American Pharmacists Association J Pharm Sci 103:1002–1012, 2014

Keywords: transdermal drug delivery; skin; passive diffusion/transport; mathematical model; *in vitro* models; formulation vehicle; diffusion

INTRODUCTION

For a topical exposure to a chemical or drug to result in a systemic exposure, the chemical (penetrant) must be absorbed across the dermal barrier. Whether in industrial or medical settings, the penetrant, in its pure form, will rarely come into contact with the skin. There is usually a vehicle that serves to solubilize the penetrant. In many cases, the permeability of the penetrant through the various layers of the skin is modulated by the constituents of the vehicle to the extent that it is the mixture that defines the ultimate level of exposure to the penetrant. Because of this interaction between the vehicle–penetrant mixture and the dermal barrier, there is marked interest in vehicle and penetrant interactions with respect to transdermal absorption.

The rate and extent of transdermal absorption depends on several characteristics of the penetrant: its partitioning into skin, diffusivity through the skin, and exposure at the skin surface.[1,2] Several studies have demonstrated the effects of vehicles on the absorption rates of topically applied compounds, by modulation of these characteristics. The permeability of halogenated methanes has been shown to be increased by up to 73-fold in corn oil compared with water.[3] In a variety of cases, the partition coefficient of the penetrant into the stratum corneum has been reported to be effected by vehicles ranging from oil, water emulsion, and petrolatum[4] to propylene glycol (PropGlyc), octonol, and ethyl decanoate[5] to isopropylmyristate.[6] Terpenes have been shown to enhance the diffusivity of 5-fluorouracil in excised epidermal membranes.[7]

Much progress has been made toward predicting transdermal absorption. Several models have been developed that take into account the chemical properties of the penetrant to describe its permeability coefficient. The original work of Potts and Guy,[8] based on a linear free-energy relationship (LFER) among molecular weight, lipophilicity, and permeability, has been further refined in more recent literature. Bunge and Cleek[9,10] have divided the Potts and Guy model into components representing resistances due to stratum corneum and epidermis. Hostynek and Magee[11] developed an LFER utilizing indicator variables to account for vehicle effects and also accounting for hydrogen bonding activity. In a comprehensive review of related literature, Abraham and Martins[12] rigorously developed a model across all of the data, utilizing descriptors for molecular size, hydrogen bonding potentials, polarity, and refractivity. An important limitation of this work, however, was that all of the compounds were exposed in an aqueous vehicle.

In the case of industrial and pharmaceutical exposure, one should also consider the effects of complex mixtures on absorption, where the multiple constituents of the vehicle may have cumulative or synergistic effects. Previous studies have demonstrated the effects of multicomponent mixtures on the rate and extent of transdermal absorption.[13–15] In particular, these metrics have been shown to be modulated by the specific composition of the vehicle. Riviere and Brooks[14,16] have used a mixture factor to account for the effect of composition of the mixture on permeability coefficient in an *in vitro* system, and total absorbed dose fraction in an *ex vivo* system. The mixture factor in these studies is a multivariate linear function that combines

Correspondence to: Jim E. Riviere (Telephone: +919-515-1912; Fax: +919-515-1909; Email: jriviere@ksu.edu)

Journal of Pharmaceutical Sciences, Vol. 103, 1002–1012 (2014)

chemical descriptors of the penetrant and vehicle constituents in a quantitative structure to property relationship (QSPR). When applied as an additive factor to the existing LFERs, the mixture factor improves the predictability of the QSPR, demonstrating the effect of the vehicle composition.[17]

Previous analyses of these, and similar, data have modeled a summary statistic of the individual absorption experiments (like permeability coefficient or fraction absorbed). That approach may lose information about how the mixture affects the absorption of the penetrant. That is, one would like to isolate the effect to modifications in partition, diffusivity, or solubility of the penetrant. The difference would be seen in the ability to predict the time course of absorption.

In a new approach to the analysis of these data, a mixed effects modeling framework is applied to simultaneously estimate parameters using all of the data within a given experimental system, while modeling the full time course of absorption. This improves the accuracy of parameter estimates by accounting for random variations, and the commonality of parameters, between experimental units. In addition, data have been collected in two different membrane systems, which should allow for the identification of common dynamics in the system not related to the membrane such as binding within the apparatus, evaporation of the vehicle, and protein binding in the receptor well.

METHODS AND MATERIALS

Experimental Apparatus

Membrane and transdermal absorption data have been collected in two experimental systems: silastic membrane flow-through diffusion cell (FTDC); porcine skin FTDC. Both experimental systems share a common set of 12 chemical penetrants in (up to) 24 vehicle combinations that are topically applied. Each system should allow for the isolation and quantification of certain dynamics of the diffusional flux. This work examines several mathematical models for the flow-through systems to accurately describe the dynamics and extent of mass transfer with the goal of explaining them in terms of penetrant and vehicle effects.

The silastic or porcine skin is punched from prepared materials (1.6 and 1.9 cm diameter, respectively) and placed into a Bronough FTDC.[18] A combination of penetrant and vehicle totaling 20 μL is applied in the donor well on the surface of the membrane. Perfusate, containing bovine serum albumin, is pumped into the receptor well at a nominal rate of 4 mL/h. The receptor well is approximately 4 mm deep and the radius of the cell is 0.45 cm. Perfusate is sampled with a frequency of every 15 min through 120 min, then every 60–480 min. The penetrant mass in perfusate is assayed by scintillation counter and converted to an observed value of flux as percent of dose per hour. Further experimental details for the porcine skin diffusion experiment are described elsewhere,[19] and the complementary silastic data are presented here for the firsttime.

Penetrants

Table 1 lists the C^{14}-tagged chemicals used as penetrants in the studies. The abbreviations shown are used in this paper.

Table 1. Chemicals Used in Treatments

Abbreviation	Chemical Name
AZ	Atrazine
CP	Chlorpyrifos
EP	Ethylparathion
FN	Fenthion
MP	Methylparathion
NP	Nonylphenol
PC	Pentachlorophenol
PH	Phenol
PN	ρ-Nitrophenol
PZ	Propazine
SZ	Simazine
TZ	Triazine

Table 2. Vehicles Used in Treatments

Eth	PG
Eth+MNA	PG+MNA
Eth+MNA+SLS	PG+MNA+SLS
Eth+PG	PG+SLS
Eth+PG+MNA	W
Eth+PG+MNA+SLS	W+MNA
Eth+PG+SLS	W+MNA+SLS
Eth+SLS	W+PG
Eth+W	W+PG+MNA
Eth+W+MNA	W+PG+MNA+SLS
Eth+W+MNA+SLS	W+PG+SLS
Eth+W+SLS	W+SLS

Eth, ethanol; MNA, methyl nicotinate; W, water; PG, propolyne glycol; SLS, sodium laureth sulfate.

Vehicles

The dosing vehicles are combinations of five constituents: ethanol (EtOH), water, PropGlyc, methyl nicotinate (MNA), and sodium lauryl sulfate (SLS). Table 2 shows the combinations of these components as used in the experimental procedures.

Modeling Approach

The goal in modeling these data is to capture the dynamics of the flux profiles in parameters that can be related to physicochemical properties of the treatments. Such parameters are likely to be mixture properties of the chemical components of the treatments, and as such should relate to a physical, as opposed to empirical, model of the membrane system. Despite the differences in the physical systems between the two membrane systems studied, silastic and porcine skin, they are modeled simultaneously to allow for shared mechanics such as boundary effects in the donor and receptor wells. This approach should add some power in isolating and identifying boundary versus membrane mechanics.

A common model is developed that describes all of the data. Each replicate in each treatment has its own unique set of parameters. The similarity of replicates within a treatment should generate similar parameters, which will correlate to chemical properties of the treatment. Finding one model that describes all of the observed data while capturing treatment effects in the parameters is the goal of this endeavor.

The model must describe three primary shapes of flux profiles. Figure 1 shows an example of each. The atrazine in ethanol profile (AZ+EtOH) is typical of many of the profiles

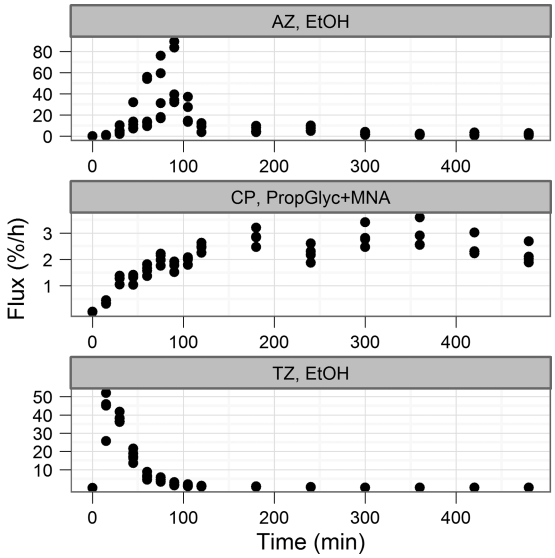

Figure 1. Flux profiles for replicates of selected treatments.

obtained in a vehicle consisting largely of ethanol in a way that there is a rapid rise to a peak flux followed by a two-phase absorption profile. The triazine in ethanol (TZ+EtOH) is similar but peaks much earlier. The profile for chlorpyrifos in propylene glycol and methylnicotinic acid (CP+PG+MNA) is very different in that the flux is low and the system appears to reach a steady state. These shapes are also exhibited by porcine skin treatments, though the fluxes are generally much lower. In short, the model must capture: lag time, maximum flux, biphasic attenuation, and quasi-steady-state behavior.

It is observed that when pure ethanol is used as a vehicle, the surface of the membrane is dry at the end of the experiment. This could indicate that the ethanol is either evaporating or penetrating the membrane. If this happens at a faster rate than the penetrant is absorbed, then the penetrant will concentrate in the donor compartment. This concentrating effect may explain the rapid rise in flux for these treatments. Models that do not account for this effect will bias the permeability estimates by inferring a low donor compartment concentration.[10] This effect may also be occurring, with less dramatic consequences, when ethanol is part of the vehicle mixture (as opposed to being the only constituent).

The mathematical models to efficiently describe (capture the dynamics and estimate parameters with good precision) each of these profiles would be significantly different. The CP+PG+MNA profile may require only a single compartment, whereas the AZ+EtOH and TZ+EtOH would require a second compartment to account for the second phase. In addition, the slow peak for AZ+EtOH and fast peak for TZ+EtOH suggest either much variability between experiments in the concentration effect of ethanol or that triazine's permeability is high enough that the concentration effect is inconsequential. So, these three profiles are representative of models that are common in a way that they all have a donor and receiver well (compartments), but differ in a way that the CP+PG+MNA profile can be described with one compartment, the TZ+EtOH with two compartments, and the AZ+EtOH with two compartments plus a concentration effect of ethanol.

As was mentioned above, previous analyses of these data have used the individual profiles to identify mean parameters by treatment. It is now proposed to use all of the data available to estimate parameters for a common model. Moreover, this common model will include random effects on the structural parameters to help quantify the differences between replicates and treatments.

The reasons for selecting against modeling the individual profiles separately are many folds. The fact that different individual profiles would require different parameters causes problems in a couple ways. The different models may indicate different rate-limiting processes between treatments. In some cases, this could cause misidentification of the parameter of interest. Given that a future goal is to produce a quantitative structure to property relationship (QSPR) for permeability and partition coefficient, accuracy in the estimates of these parameters is vital. Spurious or systematic errors in parameter estimates will degrade the precision and accuracy of QSPR predictions. Furthermore, to use the QSPR to make predictions for new penetrant and vehicle combinations, one would need to know which structural model to apply. Thus, the individual approach is not extensible.

Modeling the pooled data within a treatment, which would also be equivalent to modeling the treatments' mean flux profiles, is rejected for similar reasons. In fact, pooling the data in this way can lead to bias in parameter estimates when the differences between the replicates are not merely because of the random measurement error.

A mixed effects framework is chosen to estimate a common structural model for all of the treatments while preserving the individual estimates for each replicate. In the mixed effects framework, there is a central value for each of the model parameters. The random effects account for differences between the replicates, modifying the parameters for each profile. In identifying a structural model for the data, it is naively assumed that differences in parameter values between treatments and replicates are purely random. A flux profile that does not contain enough information to identify a parameter will drive that parameter estimate for that profile to the population median (most likely) value. The value in such a model lies in its future use to identify relationships between predictor properties and random effect estimates in the development of QSPR models.

Model Development

The data collected comprise longitudinal measurements of material flux in 288 treatments (12 compounds by 24 vehicle mixtures) with three to five replicates per treatment, all in two *in vitro* flow-through systems of silastic and porcine skin membranes. A structural model for fitting all of these data must be capable of capturing several features of individual profiles, including:

- lag time
- sharp peak
- loss of dose
- multiple terminal phases
- quasi-steady state

Figure 1 shows example profiles exhibiting one or more of these features. These dynamics may be due to the mechanisms of:

- evaporation of solvent
- loss of solute by evaporation, binding, or precipitation
- codiffusion of solvent and solute, with exhaustion of solvent
- reversible binding or partitioning within the membrane material

To capture these dynamics, a three-part model is proposed, consisting of: the donor well, the membrane, and the receptor well. This allows for separation of the mechanisms of mass transport. The donor and receptor wells are treated as well mixed compartments. The membrane is treated as either a compartmental model, or a partial differential model.

Several models that address transient diffusion have been previously published.[20–26] To minimize the number of estimated parameters, the present work uses the basic diffusion equation[27,28] for the membrane model, which treats the membrane as a homogeneous space across which the penetrant diffuses:

$$\frac{\partial C}{\partial T} = D\frac{\partial^2 C}{\partial X^2}, \quad 0 \le X \le h \tag{1a}$$

$$\frac{dM_\mathrm{d}}{dT} = DA_\mathrm{m}\left.\frac{\partial C}{\partial X}\right|_{X=0} \tag{1b}$$

$$\frac{dM_\mathrm{r}}{dT} = -DA_\mathrm{m}\left.\frac{\partial C}{\partial X}\right|_{X=h} - M_\mathrm{r}\frac{Q_\mathrm{r}}{V_\mathrm{r}} \tag{1c}$$

$$C(X, T=0) = C_0(1 - H(x)) \tag{1d}$$

The model comprises equations for: the mass transport of penetrant through the membrane (Eq. 1a), which is the partial differential equation (PDE) for diffusion; the boundary conditions at the donor well (Eq. 1b) and receptor well (Eq. 1c); and the initial condition within the membrane (Eq. 1d). The independent variables are time (T) and distance in the membrane (X) ranging from 0 to h. The dependent variables are the concentration in the membrane (C), the mass in the donor well (M_d), and the mass in the receptor well (M_r). The parameters are diffusivity (D), cross-sectional area of the membrane (A_m), receptor well volume, and perfusion rate (V_r, Q_r). The initial condition, where H is the Heaviside function, specifies a zero concentration everywhere in the membrane at $T = 0$ except at the boundary at $X = 0$, where it is some initial concentration (C_0).

Equation 1a can be modified to account for reversible binding within the membrane by augmenting the system.[28–30] If bound penetrant is presumed to be spatially stationary and the binding is treated as a volume reaction, the PDE in Eq. 1a is modified by adding a dependent variable for the bound concentration in the membrane ($F(X, T)$) and accounting for forward and backward transfer of penetrant according to rate constants k_f and k_b:

$$\frac{\partial C}{\partial T} = D\frac{\partial^2 C}{\partial X^2} - k_\mathrm{f}C + k_\mathrm{b}F \tag{2a}$$

$$\frac{\partial f}{\partial T} = k_\mathrm{f}C - k_\mathrm{b}F \tag{2b}$$

The donor well boundary condition in Eq. 1b can be rewritten considering wetted membrane area (A_d), donor well volume (V_d) as functions of time, and assuming instantaneous equilibration with partition coefficient (K_dm) at the membrane boundary ($C_0 = K_\mathrm{dm}C_\mathrm{d}$) to get the membrane boundary condition:

$$\frac{\partial C}{\partial T} + \frac{C}{V_\mathrm{d}}\frac{dV_\mathrm{d}}{dT} - \frac{K_\mathrm{dm}A_\mathrm{d}D}{V_\mathrm{d}}\frac{\partial C}{\partial X} = 0\Big|_{X=0} \tag{3}$$

Similarly, the receptor well mass balance yields a boundary condition that incorporates a partition coefficient (K_rm), the membrane area (A_m), and a binding coefficient such that $C|_{x=h} = f_\mathrm{u}K_\mathrm{rm}C_\mathrm{r}$, and the receptor well Eq. 1c becomes:

$$\frac{\partial C}{\partial T} + \frac{f_\mathrm{u}K_\mathrm{rm}A_\mathrm{m}D}{V_\mathrm{r}}\frac{\partial C}{\partial X} + \frac{Q}{V_\mathrm{r}}C = 0\Big|_{X=h} \tag{4}$$

Note that if the fraction unbound $f_\mathrm{u} = 0$, then there is a Dirichlet boundary at the receptor with $C(h, T) = 0$.

Several simplifications have been made in this model. Equation system 1a–1a is simplified by taking diffusivity only as a function of time, not position in the membrane, so diffusivity changes with time uniformly at all locations in the membrane. The model considers only one membrane barrier, rather than two membranes in series, which is a more physiologically relevant description of the porcine skin system.[9,10] The single-membrane model would be a reasonable approximation as long as one of the physiological membranes dominates the resistance. That is, the single membrane model could work well for compounds that transit quickly through either the stratum corneum or the viable epidermis, but would be less accurate in cases where resistance in both regions of the skin are similar. Finally, none of the parameters of the model are taken to be functions of concentration of the vehicle or penetrant.

Nondimensionalizing the equations makes them easier to work with. In general, working with the nondimensional form makes tuning the integrator simpler. In the case of equation system 2a and 2b, a parameter is eliminated making the model uniquely estimable. The dimensionless form for equation system 1a–1a is given by the system of Eqs. 5a–5d, with nondimensional variables written in lower case:

$$\frac{\partial c}{\partial t} = \frac{\partial^2 c}{\partial x^2}, \quad x \in [0, 1], \quad t \le 0 \tag{5a}$$

$$\left[\frac{\partial c}{\partial t} - K_\mathrm{1d}\frac{\partial c}{\partial x} + K_\mathrm{2d}c = 0\right]_{x=0} \tag{5b}$$

$$\left[\frac{\partial c}{\partial t} - K_\mathrm{1r}\frac{\partial c}{\partial x} + K_\mathrm{2r}c = 0\right]_{x=1} \tag{5c}$$

$$c(x, 0) = 1 - H(x), \quad x \in [0, 1] \tag{5d}$$

The terms in the boundary conditions have been condensed into constants K_1d, K_2d, K_1r, and K_2r. Nondimensionalization of equation system 2a and 2b with the relations $K = \frac{k_\mathrm{f}}{k_\mathrm{b}}$ and $k_\mathrm{b} = \frac{D}{h^2}$ eliminates a parameter from the model.

$$\frac{\partial c}{\partial t} = \frac{\partial^2 c}{\partial x^2} - K(c - f) \tag{6a}$$

$$\frac{\partial f}{\partial t} = c - f \tag{6b}$$

This simplification fixes a relationship between D and k_b, making the model estimable from the flux data. The implied assumption is that the flux is a measure of the slower of the diffusion coefficient and backward rate constant, if they differ by orders of magnitude, or a combination of the two, if they are of similar magnitude. A study[30] of theophylline diffusion through stratum corneum used a binding model similar to Eq. 2a, but fixed the value for K from previous data to identify k_f and k_b. Interpretation of the results shows that $k_b h^2/D \neq 1$ for that experiment. The choice of fixing the relationship between D and k_b rather than fixing K, which would require additional data, introduces bias into the parameter estimates. So, even if the model given by Eqs. 6a and 6b fits the data well, the parameter estimates should be interpreted cautiously.

The linear system of Eq. 5a has an analytical solution for the case where all of the coefficients are constant. For cases with nonlinearities or variable coefficients, one must resort to numerical methods for the solution of the equations. The method of lines (MOL)[31] approach is used whereby the spatial differentials are discretized, leaving a system of $N + 1$ ordinary differential equations for each of the membrane PDEs, where N is the number of discrete divisions of the spatial dimension of the membrane.

Using forward differences for the first-order partial derivatives,

$$\frac{\partial c}{\partial x} = \frac{c_{i+1} - c_i}{\Delta x} \tag{7a}$$

$$\frac{\partial^2 c}{\partial x^2} = \frac{c_{i+1} - 2c_i + c_{i-1}}{\Delta x^2} \tag{7b}$$

Equations 5a and 6a are approximated as Eqs. 8 and 9a, where i $(0 < i < N)$ denotes the node of the discretization.

$$\frac{dc_i}{dt} = \frac{c_{i+1} - 2c_i + c_{i-1}}{\Delta x^2} \tag{8}$$

$$\frac{dc_i}{dt} = \frac{c_{i+1} - 2c_i + c_{i-1}}{\Delta x^2} - K(c_i - f_i) \tag{9a}$$

$$\frac{df_i}{dt} = c_i - f_i \tag{9b}$$

The boundary conditions are given by:

$$\frac{dc_0}{dt} = K_{1d}\frac{c_1 - c_0}{\Delta x} - K_{2d}c_0 \tag{10a}$$

$$\frac{dc_N}{dt} = K_{1r}\frac{c_N - c_{N-1}}{\Delta x} - K_{2r}c_N \tag{10b}$$

The discretized system approximates the solution to the PDEs with increasing accuracy as N increases. The MOL solution for various values of N is compared with the analytical solution in Figures 2–4. The discretized system for $N = 1$ corresponds to an instantly equilibrated membrane with a linear concentration profile. This system would be unable to account for time lag because the initial flux must be nonzero. The root mean square error (RMSE) values for each N are tabulated in Table 3. The relative bias in estimating the diffusion coefficient with the discretized model shows increasing accuracy as N increases. In the interest of saving computational time in estimating parameters for the models, the lowest value for N that maintains reasonable accuracy should be used. The timing for 100 simulations, relative to the case for $N = 1$ shows a dramatic increase in run time at $N > 50$, whereas $N = 20$ provides a balance of accuracy and speed for parameter estimation.

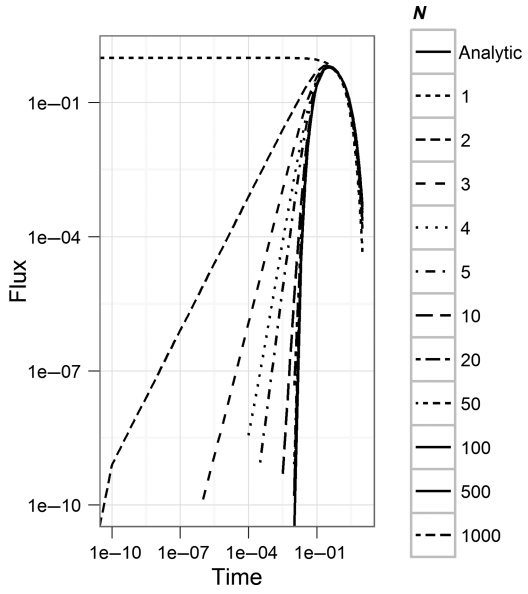

Figure 2. Comparison of analytic and MOL predictions for Eq. 5a.

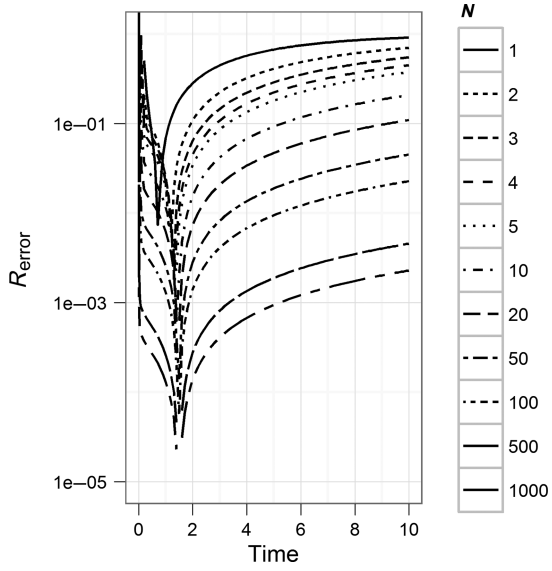

Figure 3. Comparison of analytic and MOL relative error for Eq. 5a.

Models

Four models are derived using the discretized membrane model and boundary conditions above. In the models below, y_{ij} and f_{ij} are the observed and predicted flux for profile i at time j. Random effects are denoted with a preceding $\eta$and are taken to

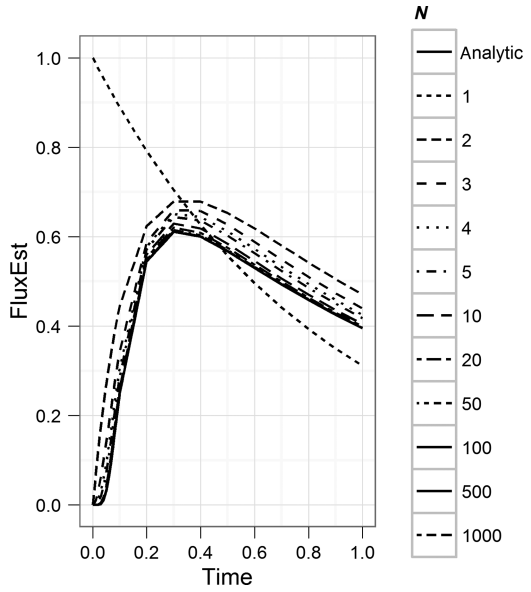

Figure 4. Comparison of estimated profiles from MOL approximation to analytic profile of Eq. 5a.

Table 3. Bias in Estimated Diffusion Coefficient, RMSE, and Relative Timing for Values of N Approximating Eq. 5a

N	Relative Bias	RMSE	Relative Timing
1	1.438e–01	4.433e–01	1.000
2	−2.131e–01	7.125e–02	1.000
3	−1.094e–01	3.553e–02	1.182
4	−6.748e–02	2.208e–02	1.727
5	−4.650e–02	1.546e–02	1.636
10	−1.528e–02	5.675e–03	2.545
20	−5.571e–03	2.437e–03	3.818
50	−1.732e–03	9.070e–04	7.545
100	−7.846e–04	4.452e–04	15.000
500	−1.436e–04	8.779e–05	132.818
1000	−7.119e–05	4.382e–05	256.364

be normally distributed with covariance matrix Ω. The residuals ε_{ij} (difference between predicted and observed flux) are assumed to be independently and normally distributed with mean zero and variance $\left(a + bf_{ij}\right)^2$. A partition coefficient from the vehicle to the membrane (K_{sm}) is confounded with C_0 and D, so for this work partitioning is subsumed in the diffusivity parameter (D).

Model 100

Model 100 incorporates Eqs. 8 and 10a to predict flux. It is parameterized by diffusivity (D) and fraction of dose available for permeation (F). Fixed effects are incorporated (D_{mat} and F_{mat}) to describe the difference in diffusivity and availability in the different materials. Random effects are incorporated in D and F, which are taken to be distributed log-normally and inverse logistically, respectively.

$$y_{ij} = f_{ij}\left(F_i, D_i, t_j\right) + \varepsilon_{ij} \tag{11a}$$

$$F_i = \frac{1}{1 + e^{-\left(F + F_{\mathrm{mat}} + \eta_{F_i}\right)}} \tag{11b}$$

$$D_i = e^{\left(D + D_{\mathrm{mat}} + \eta_{D_i}\right)} \tag{11c}$$

Model 200

Model 200 incorporates Eqs. 9a and 10a to predict flux. It is parameterized as Model 100, with the addition of the partition coefficient parameter K, and the removal of F_{mat}. The partition coefficient is log-normally distributed with a random effect and a fixed effect for material (K_{mat}).

$$y_{ij} = f_{ij}\left(F_i, D_i, K_i, t_j\right) + \varepsilon_{ij} \tag{12a}$$

$$F_i = \frac{1}{1 + e^{-\left(F + \eta_{F_i}\right)}} \tag{12b}$$

$$D_i = e^{\left(D + D_{\mathrm{mat}} + \eta_{D_i}\right)} \tag{12c}$$

$$K_i = e^{\left(K + K_{\mathrm{mat}} + \eta_{K_i}\right)} \tag{12d}$$

Model 120

Model 120 is a modification of Model 100 to include a dynamic change in diffusivity due to the vehicle effects. Diffusivity is multiplied by a positive factor D_{dyn} during a time range parameterized by an onset time T_{on} and duration T_{dur}. These additional parameters incorporate random effects in a log-normal distribution. The material effect on dose availability (F_{mat}) is removed.

$$y_{ij} = f_{ij}\left(F_i, D_i, t_j\right) + \varepsilon_{ij} \tag{13a}$$

$$F_i = \frac{1}{1 + e^{-\left(F + \eta_{F_i}\right)}} \tag{13b}$$

$$D_i(t) = e^{\left(D + D_{\mathrm{mat}} + \eta_{D_i} + \eta_{D_{\mathrm{dyn},i}}\left(t_{\mathrm{on},i} < t < t_{\mathrm{dur},i}\right)\right)} \tag{13c}$$

$$t_{\mathrm{on},i} = t_{\mathrm{on}} e^{\eta_{t_{\mathrm{on},i}}} \tag{13d}$$

$$t_{\mathrm{dur},i} = t_{\mathrm{dur}} e^{\eta_{t_{\mathrm{dur},i}}} \tag{13e}$$

Model 220

Model 220 makes the same modifications to Model 200 as Model 120 makes to Model 100.

$$y_{ij} = f_{ij}\left(F_i, D_i, K_i, t_j\right) + \varepsilon_{ij} \tag{14a}$$

$$F_i = \frac{1}{1 + e^{-\left(F + \eta_{F_i}\right)}} \tag{14b}$$

$$K_i = e^{\left(K + K_{\mathrm{mat}} + \eta_{K_i}\right)} \tag{14c}$$

$$D_i(t) = e^{\left(D + D_{\mathrm{mat}} + \eta_{D_i} + \eta_{D_{\mathrm{dyn},i}}\left(t_{\mathrm{on},i} < t < t_{\mathrm{dur},i}\right)\right)} \tag{14d}$$

$$t_{\mathrm{on},i} = t_{\mathrm{on}} e^{\eta_{t_{\mathrm{on}},i}} \tag{14e}$$

$$t_{\mathrm{dur},i} = t_{\mathrm{dur}} e^{\eta_{t_{\mathrm{dur}},i}} \tag{14f}$$

Computation

There is a limited selection of nonlinear mixed effects modeling software available for the use for problems such as this. Regardless of the software chosen, the majority of the computational time is used in the evaluation of the objective function, which for complicated differential equation models means the prediction of the individual profiles. This is a task that can be parallelized. Because of the limitations on the size of the equation system in some tools, and lack of parallelization in others, a tool was chosen that would allow one to implement the prediction as efficiently as possible.

The equations were implemented in C++, using the SUNDIALS CVODE solver.[32] The interface was designed such that all of the individual profiles are computed in a single call. The predictions for the individual profiles are split across the available computing cores on a single machine using OpenMP. The C++ library is dynamically linked with the R statistical software platform,[33] and the estimation accomplished with the SAEM algorithm provided by the saemix package[34] for R. Computations were carried out on a dual chip Intel Xeon processor with a total of eight cores.

Convergence of the algorithm was established by viewing plots of log-likelihood and parameter values over the iteration history to ensure that they enter a stable distribution during burn in and solve within said distribution. The log-likelihood, AIC, and BIC are computed by importance sampling. Standard errors of the estimates come from the Fisher Information Matrix, computed by linearization. Maximum a posteriori (MAP) estimates of the random effects and individual parameters are computed by regression. The MAP estimates are used to predict the individual profiles.

RESULTS

Four models were assessed for goodness of fit: the simple membrane (Model 100), the membrane with binding (Model 200), and both with dynamics on diffusivity (Models 120 and 220). Each of the four models was estimated with both a diagonal-only and full covariance matrix for the random effects. The flux observations for the porcine skin membranes were orders of magnitude lower than those for the silastic membranes. A constant variance error model resulted in poor fits for the porcine skin data, whereas an exponential model resulted in poor fits for the silastic data with high peak values. A combined additive plus proportional error model worked well across the models and allowed a good comparison of model predictions.

Model 100 worked well for predicting peak fluxes in many of the silastic cells. There were several treatments for which the more sharply defined peaks (common with treatments containing EtOH) were severely under predicted. In addition, many of the low flux profiles (flux $<$ 2% dose/h) were very poorly predicted.

Model 200 predicted the apparent two-phase flux of some of the profiles quite well, with binding allowing for an extended half-life of the flux profile. Some of the sharper peaks still were poorly estimated, but the low flux profiles were estimated with much higher precision.

Model 120 included a dynamic diffusivity and provided substantial improvement in fit based on RMSE and R^2. Subjectively, it radically improved the fit of the sharp peaks and tails of nearly all profiles.

Model 220, like Model 120, improved the fit greatly as compared with Models 100 and 200. It has the lowest values for R^2 and RMSE so appears to fit this dataset the best, though differences in individual profiles from Model 120 are not generally apparent.

The limited dose availability parameter (F) describes loss of penetrant through a secondary pathway such as evaporation or irreversible binding. The parameter is constrained by logistic transformation to values between 0 and 1, and allows the models to fit profiles where the total accumulated flux (area under the curve) is less than 100% of the dose. It is especially important for profiles where the flux profile is decaying but the total absorption is low. Model 100 only fit well when a material effect was added to dose availability. The other models did not suffer when the material effect was removed and the variance of the random effect on F was unchanged. Attempts to fit Models 200 and 220 with a fixed dose availability of 100%, to attribute low flux to the partition coefficient, resulted in poor fits to the data.

Figure 5 shows the MAP predicted values for each replicate of the treatments noted above. Only the fits for the diagonal covariance are shown as they are virtually indistinguishable from those for the full covariance. The models with the dynamic diffusivity (120, 220) show a remarkably better fit to the data with sharp peaks. The change in diffusivity is necessary to accommodate both lag and the high peak in the AZ,EtOH,SI treatment. Partitioning (Models 200, 220) helps with the CP,PropGlyc+MNA,SI profile, but is not readily distinguishable from the Model 120 fit.

Overall performance of the models is assessed in Figure 6. Models 120 and 220 show the best agreement between the observed and MAP predicted flux values, whereas Models 100 and 200 show much more dispersion. Table 4 shows the goodness of fit statistics for the models. Note that AIC and BIC overwhelmingly support Model 220 with full covariance as the best fit. Table 5 gives the parameter estimates for the fixed effects. Table 6 gives the variance–covariance matrix of the random effects and shows the post hoc shrinkage in the final row.

DISCUSSION

All of the models investigated capture the time lag exhibited by the data. Initial experiments with compartmental models and diffusion models with fewer spatial discretization points performed poorly in this regard. The simplest model investigated (Model 100) fails to account for sharp peaks and long half-lives, especially when these two characteristics appear within the same treatment. The addition of intramembrane binding helps somewhat with these, but the dynamic diffusivity models (Models 120 and 220) capture the sharp peaks best.

The random effect on diffusivity should account for vehicle effects between treatments, so the improved fit with the dynamic diffusivity models indicates that at least for some treatments, the effect is either temporary or slowly accumulating. Time-dependent effects due to vehicle comprising EtOH have been reported in the literature.[5] Modulation of penetrants'

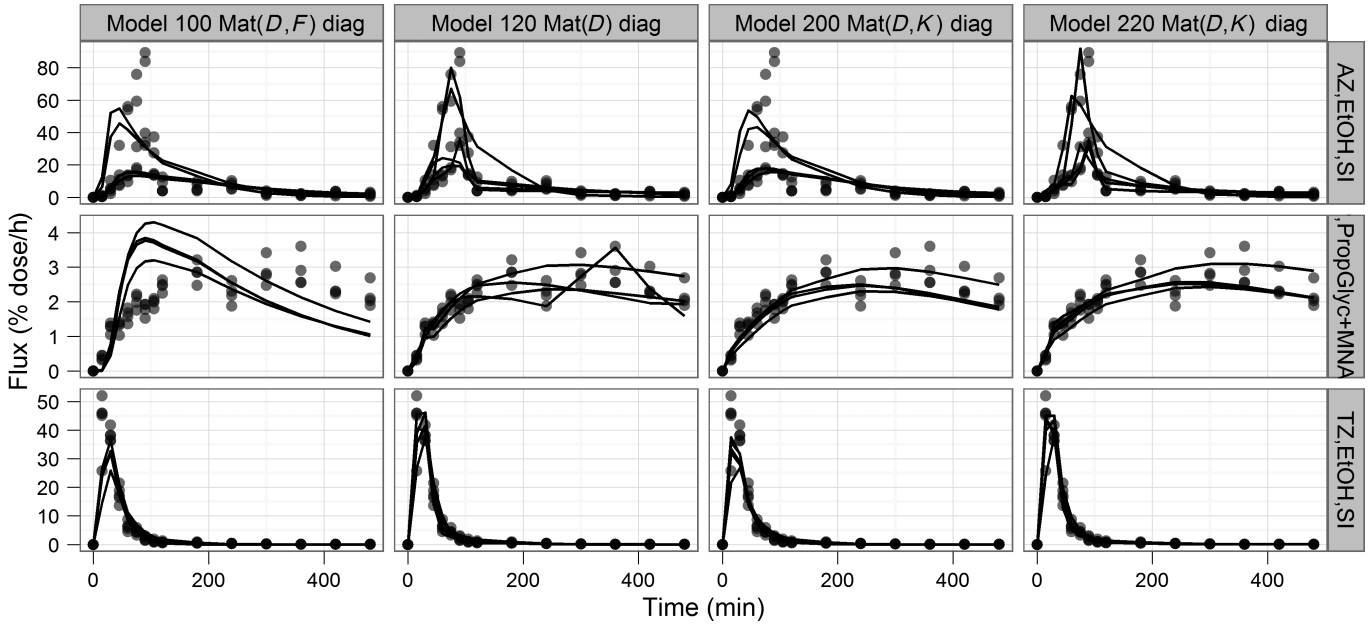

Figure 5. Model fits for selected treatments.

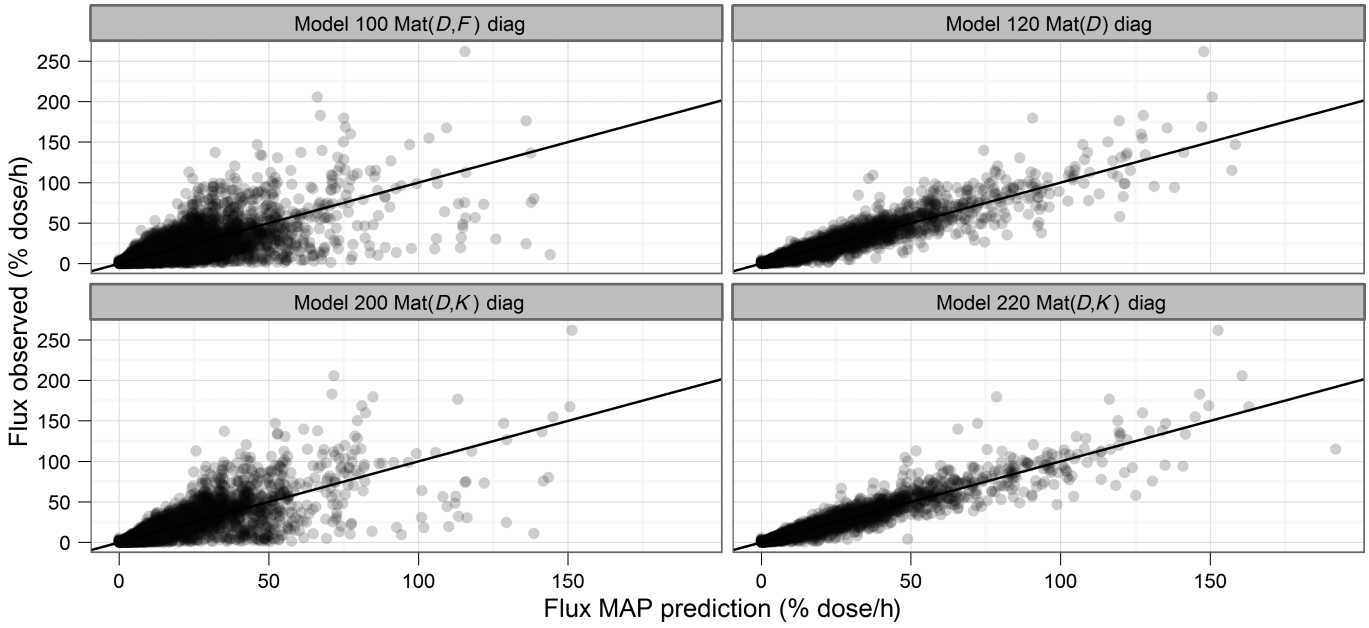

Figure 6. MAP estimated flux versus observed flux.

Table 4. Model Fit Statistics

Model	−2LL	AIC	BIC	R^2	RMSE	NPAR
Model 100 Mat(*D*,*F*) diag	82,356	82,372	82,419	0.629	6.23	8
Model 100 Mat(*D*,*F*) full	82,312	82,330	82,383	0.629	6.24	9
Model 120 Mat(*D*) diag	52,202	52,226	52,296	0.930	2.63	12
Model 120 Mat(*D*) full	50,787	50,831	50,960	0.923	2.75	22
Model 200 Mat(*D*,*K*) diag	62,753	62,773	62,832	0.757	4.87	10
Model 200 Mat(*D*,*K*) full	61,275	61,301	61,378	0.770	4.76	13
Model 220 Mat(*D*,*K*) diag	47,793	47,823	47,911	0.940	2.41	15
Model 220 Mat(*D*,*K*) full	45,953	46,013	46,189	0.943	2.36	30

−2LL, −2*Log Likelihood; AIC, akaike information criterion; BIC, Bayesian information criterion; R^2, coefficient of determination; RMSE, root mean square error; NPAR, number of fitted parameters.

Table 5. Fixed Effect Parameter Estimates for Model 220

Parameters	Estimate	SE
F	5.374e − 01	1.270e − 02
Diff	3.143e − 05	1.064e − 06
beta_MatIDPS(Diff)	1.540e + 00	6.315e − 02
K	2.775e + 00	1.374e − 01
beta_MatIDPS(K)	4.819e + 00	7.911e − 02
D_{dyn}	0.000e + 00	0.000e + 00
t_{on}	4.787e + 00	2.791e − 01
t_{dur}	1.739e + 02	5.191e + 00
a	8.747e − 02	5.193e − 04
b	1.769e − 01	2.693e − 08

diffusivity by codiffusing permeability enhancers in the dosing vehicle have been anticipated as well.[26,35]

The use of a mixed effects model to tease out the differences in parameter values between treatments is powerful and convenient. It is powerful because it can capture the variability within treatments as well as between treatments. The convenience comes from not having to postulate individual models per treatment or specify initial estimates for each profile, as would be necessary if modeled individually. However, the use of more complicated models than required for many treatments combined with the use of random effects on the structural parameters raises the specter of over fitting. One would expect that the treatments that may be well described by model 100 would show regression to the mean when fit with Model 220. There is a subset of treatments that is driving the estimation of the additional parameters in more complicated models. These effects lead to shrinkage in the a posteriori parameter estimates that limit their utility in covariate model building and inference.[36] In addition, the simplification in Eq. 6a introduces bias into the parameters. Therefore, although the current analysis is useful for identifying models that can describe the data, it is probably not useful for identifying particular parameter values within groups of treatments.

The plot of individual predictions versus observations in Figure 6 clearly shows better agreement for Models 120 and 220, which both have the dynamic diffusion terms added. They also almost always fit the data with high peaks better than the other models.

As the models become more complex, the ability to identify the parameters is potentially reduced. The dynamic diffusion term may be confounded with the partition coefficient in a way that both can be used to describe a flux profile with two terminal phases. There are few treatments with high peaks and a second phase where both parameters would be uniquely identified. This may explain why these two models are so similar in their diagnostics. The randomness in the onset and duration of the dynamics as well the size of the effect on diffusivity are probably the main source of over fitting.

The choice of error model has a dramatic effect on the ability to fit the models. This has much to do with the structure of the data. Some of the treatments exhibit very low fluxes along their entire profile (e.g., flux < 1%/h), whereas others show high peaks followed by low plateaus. The fact that many profiles show exclusively low profiles means that additive models will generally ascribe such measurements to pure noise while proportional error models will fit them at the expense of the large peaks; at least in the face of model misspecification. The combined error model used this analysis mostly avoided the worst of the additive and proportional behavior, but still is not optimal. Although the combined model establishes a fixed error at low fluxes and a proportional error at high fluxes, the desired behavior based on sensitivity of the assay and adjustments for baseline levels may indicate a fixed error at high flux and a proportional error at low fluxes. In addition, the ability to adjust the error level based on the membrane system used in the treatment may be useful as the majority of low flux profiles are observed in the porcine skin system. Limitations in the software used for this analysis made such an option inaccessible, but it would be worthwhile in the future to switch software as the improved precision in estimation should improve the estimates of the parameters and increase the utility of the lower flux data in the models.

CONCLUSIONS

Four different models of flux in flow-through membrane cells have been tested to assess their ability to fit the data from treatments consisting of permutations of 24 vehicle mixtures and 12 penetrants in two membrane systems. A mixed effects modeling framework has been applied so that models can be estimated with as few fixed effect parameters as possible, whereas also quantifying variability and accounting for correlation in the data. The models account for diffusion and binding within the membrane as well as dynamics on the diffusion coefficient, without making many assumptions about the mechanisms of those dynamics. To varying degrees, the models explain key features of the data, such as: lag time, sharp peaks in flux, two terminal phases, and low flux profiles.

The models with dynamic diffusivity fit the data much better than those without, particularly with respect to the sharp peaks. There is overwhelming support for models that include intramembrane binding, particularly when comparing within the class of models that also include dynamic diffusivity. The ability to capture the low flux profiles is a function of a dose availability parameter that was tested in various models and included in all models presented here. The data originate from

Table 6. Estimated Random Effect Covariance Matrix for Model 220

	F	Diff	K	D_{dyn}	t_{on}	t_{dur}
F	4.2819	0.2076	−0.5263	0.0302	−1.0692	0.0405
Diff	0.2076	1.4032	0.9404	−0.0944	−0.0264	0.1070
K	−0.5263	0.9404	2.6668	−0.1781	−0.1256	0.0647
D_{dyn}	0.0302	−0.0944	−0.1781	1.1046	0.7994	0.1495
t_{on}	−1.0692	−0.0264	−0.1256	0.7994	3.1024	0.6780
t_{dur}	0.0405	0.1070	0.0647	0.1495	0.6780	1.3577
Shrinkage	0.1668	0.2280	0.1843	0.1929	0.3142	0.3655

two different membrane systems with very different fluxes, which the models address by using a combined proportional plus constant error model.

Further work to add covariate effects as functions of chemical properties of the penetrants and vehicle constituents should focus on models that incorporate dynamics on the diffusivity. Concerns about over fitting could be diminished by searching for structural models for such dynamics that relate to the physical mechanisms in action. Additional data should also be introduced to fix some parameters of the model to improve estimability while preserving physical meaning of the parameters.

The mixed effects modeling approach explored in this work provides a framework for combining data from different experiments and handling the diverse sources of variability. This may be a powerful approach for linking data in multiscale experiments, where different experiments are optimized to differentiate components of the absorption process. Such an approach could relate *in vitro* experimental data to *in vivo* observations and provide a platform for extrapolating *in vitro* assays to *in vivo* predictions with an emphasis on projecting potential variability.

ACKNOWLEDGMENT

Funding for this research was provided by National Institute of Occupational safety and Health Grant (R01 07555).

REFERENCES

1. Moser K, Kriwet K, Naik A, Kalia YN, Guy RH. 2001. Passive skin penetration enhancement and its quantification in vitro. Eur J Pharm Biopharm 52(2):103–112.
2. Wiechers JW. 1989. The barrier function of the skin in relation to percutaneous absorption of drugs. Pharm World Sci 11(6):185–198.
3. Jepson G, McDougal J. 1999. Predicting vehicle effects on the dermal absorption of halogenated methanes using physiologically based modeling. Toxicol Sci 48(2):180–188.
4. Chatelain E, Gabard B, Surber C. 2003. Skin penetration and sun protection factor of five UV filters: Effect of the vehicle. Skin Pharmacol Appl Skin Physiol 16(1):28–35.
5. Hatanaka T, Katayama K, Koizumi T, Sugibayashi K, Morimoto Y. 1995. Time-dependent percutaneous absorption enhancing effect of ethanol. J Control Release 33(3):423–428.
6. Surber C, Wilhelm K-P, Hori M, Maibach HI, Guy RH. 1990. Optimization of topical therapy: Partitioning of drugs into stratum corneum. Pharm Res 7(12):1320–1324.
7. Williams AC, Barry BW. 1991. Terpenes and the lipid–protein-partitioning theory of skin penetration enhancement. Pharm Res 8(1):17–24.
8. Potts RO, Guy RH. 1992. Predicting skin permeability. Pharm Res 9(5):663–669.
9. Bunge AL, Cleek RL. 1995. A new method for estimating dermal absorption from chemical exposure: 2. Effect of molecular weight and octanol-water partitioning. Pharm Res 12(1):88–95.
10. Cleek RL, Bunge AL. 1993. A new method for estimating dermal absorption from chemical exposure. 1. general approach. Pharm Res 10(4):497–506.
11. Hostynek J, Magee P. 1997. Modelling in vivo human skin absorption. Quant Struct Act Relat 16(6):473–479.
12. Abraham MH, Martins F. 2004. Human skin permeation and partition: General linear free-energy relationship analyses. J Pharm Sci 93(6):1508–1523.
13. Qiao GL *et al*. 1996. The use of mechanistically defined chemical mixtures (MDCM) to assess component effects on the percutaneous absorption and cutaneous disposition of topically exposed chemicals: I. Studies with parathion mixtures in isolated perfused porcine skin. Toxicol Appl Pharmacol 141(2):473–486.
14. Riviere JE, Brooks JD. 2011. Predicting skin permeability from complex chemical mixtures: Dependency of quantitative structure permeation relationships on biology of skin model used. Toxicol Sci 119(1):224–232.
15. Rosado C, Cross SE, Pugh WJ, Roberts MS, Hadgraft J. 2003. Effect of vehicle pretreatment on the flux, retention, and diffusion of topically applied penetrants in vitro. Pharm Res 20(9):1502–1507.
16. Riviere J, Brooks J. 2007. Prediction of dermal absorption from complex chemical mixtures: Incorporation of vehicle effects and interactions into a QSPR framework. SAR QSAR Environ Res 18(1-2):31–44.
17. Ghafourian T, Samaras EG, Brooks JD, Riviere JE. 2010. Modelling the effect of mixture components on permeation through skin. Int J Pharm 398(1–2):28–32.
18. Chang SK, Riviere JE. 1991. Percutaneous absorption of parathion in vitro in porcine skin: Effects of dose, temperature, humidity, and perfusate composition on absorptive flux. Fundam Appl Toxicol 17(3):494–504.
19. Riviere J, Brooks J. 2005. Predicting skin permeability from complex chemical mixtures. Toxicol Appl Pharmacol 208(2):99–110.
20. Barbero AM, Frasch HF. Modeling of diffusion with partitioning in stratum corneum using a finite element model. Ann Biomed Eng 33(9):1281–1292.
21. Dancik Y, Miller MA, Jaworska J, Kasting GB. 2013. Design and performance of a spreadsheet-based model for estimating bioavailability of chemicals from dermal exposure. Adv Drug Deliv Rev 2(0):221–236.
22. Frasch HF, Barbero AM. 2008. The transient dermal exposure: Theory and experimental examples using skin and silicone membranes. J Pharm Sci 97(4):1578–1592.
23. Kasting GB. 2001. Kinetics of finite dose absorption through skin 1. Vanillylnonanamide. J Pharm Sci 90(2):202–212.
24. Kasting GB, Miller MA, Bhatt VD. 2008. A spreadsheet-based method for estimating the skin disposition of volatile compounds: Application to N,N-diethyl-m-toluamide (DEET). J Occup Environ Hyg 5(10):633–644.
25. Krüse J *et al*. 2007. Analysis, interpretation, and extrapolation of dermal permeation data using diffusion-based mathematical models. J Pharm Sci 96(3):682–703.
26. Rim J, Pinsky P, Osdol W. 2005. Finite element modeling of coupled diffusion with partitioning in transdermal drug delivery. Ann Biomed Eng 33(10):1422–1438.
27. Anissimov YG, Roberts MS. 1999. Diffusion modeling of percutaneous absorption kinetics. 1. Effects of flow rate, receptor sampling rate, and viable epidermal resistance for a constant donor concentration. J Pharm Sci 88(11):1201–1209.
28. Mitragotri S *et al*. 2011. Mathematical models of skin permeability: An overview. Int J Pharm 418(1):115–129.
29. Anissimov YG, Roberts MS. 2009. Diffusion modelling of percutaneous absorption kinetics: 4. Effects of a slow equilibration process within stratum corneum on absorption and desorption kinetics. J Pharm Sci 98(2):772–781.
30. Frasch HF, Barbero AM, Hettick JM, Nitsche JM. 2011. Tissue binding affects the kinetics of theophylline diffusion through the stratum corneum barrier layer of skin. J Pharm Sci 100(7):2989–2995.
31. Schiesser WE, Griffiths GW. 2009. Compendium of partial differential equation models: Method of lines analysis with Matlab. New York City, New York: Cambridge University Press.
32. Hindmarsh AC *et al*. 2005. SUNDIALS: Suite of nonlinear and differential/algebraic equation solvers. ACM Trans Math Softw 31(3):363–396.

33. Team RDC. 2012. R: A language and environment for statistical computing. Vienna, Austria: R Foundation for Statistical Computing.
34. Comets E, Lavenu A, Lavielle M. 2011. saemix: Stochastic approximation expectation maximization (SAEM) algorithm.
35. Manitz R, Lucht W, Strehmel K, Weiner R, Neubert R. 1998. On mathematical modeling of dermal and transdermal drug delivery. J Pharm Sci 87(7):873–879.
36. Savic R, Karlsson M. 2009. Importance of shrinkage in empirical bayes estimates for diagnostics: Problems and solutions. AAPS J 11(3):558–569.